

Effect of high level differential heating on failure of encapsulated Chips and Semiconductors

Ashraf Balabel and Ismail Sakr^c

*Mechanical Power Engineering Department, Faculty of Engineering
Menoufia University - Shebin El-kom, EGYPT.*

Received: 04/08/2011 – Revised 11/04/2012 – Accepted 20/04/2012

Abstract

Chip encapsulation on printed circuit boards (PCB) requires an accurate amount of encapsulation material to protect the chip in semiconductor packaging. Encapsulation materials are usually made of epoxy but sometimes other materials are used, like silicones. The study of convective flows and heat transfers in such systems of immiscible liquid layers has a great potential. In the current investigation, the failure criteria of the encapsulated chips subjected to high level of differential heating is numerically defined. The Reynolds-Averaged Navier-Stokes equations along with energy equation are solved on the basis of the control volume approach. The level set formulation is applied to smooth the discontinuous properties of the encapsulated layers and to predict the dynamics of the separation surface between the two layers. The numerical results obtained showed that most of the failure occurs in encapsulated chips and semiconductors are referred to the deformation of the separation surface especially at high level of differential heating.

Keywords: Chips encapsulation; numerical simulation; thermocapillary convection; turbulent flow; level set method; two-layer system.

1. Introduction

Chips are small electronic circuits, also known as integrated circuits, which are one of the basic components of most kinds of electronic devices, especially computers. Computer chips are small and are made of semiconductors that are usually composed of silicon, on which several tiny components including transistors are embedded and used to transmit electronic data signals. They became popular in the latter half of the 20th century because of their small size, low cost, high performance and ease to produce. Moreover, the micro-electronic revolution resulted in the fact that nowadays semi-conductor chips can be found in nearly all devices in our surroundings. Also, electronic components in the automotive sector and in high-quality industrial products, such as controls, are subjected to extreme conditions as they are operated in a wide temperature range of use. Therefore, different packaging techniques have been developed in order to operate these devices in a secure and reliable manner during their entire service lives.

Multi-layer chips and semiconductors have to go through an assembly and interconnection process, i.e. by adhesive or solder on e.g. a copper lead-frame, followed by an encapsulation

^c Corresponding Author: Ismail Sakr

Email: ismailsakr@yahoo.com Telephone: +2-048-2333081

© 2009-2012 All rights reserved. ISSR Journals

Fax: +2-048-2235695

PII: S2180-1363(10)4254-X

process, as shown in Fig. 1. All of that pose potential reliability risks to the chips' structural integrity. Chips are known to fail due to failures caused during manufacture or extrinsic failure induced by thermal processing [1], as damage can lead to encapsulant material migration and much later to fatal failure by electrical shorts.

The Study of interfacial convection in systems of immiscible liquid layers with interfaces is a widespread phenomenon that is of great importance in numerous branches of technology, including chemical engineering, space technologies, coating, etc [2]. Scientific interest in such systems is due to the fact that the interfacial convection in multilayer systems is characterized by a variety of physical mechanisms and types of instability.

In multi-layer systems, the convection induced by the Marangoni effect, i.e. by a surface stress due to the variation of surface tension with temperature along an interface or a surface, is of major importance [3]. In the process of crystal growth, encapsulation of an electric melt is used to control melt stoichiometry when the melt contains a volatile component [4]. Moreover, encapsulation can be useful for a better control of heat transfer [5]. In addition, it also has the advantage of reducing or even eliminating the convective flow in the melt, hence drastically reducing the unwanted inhomogeneities in solidifying materials. The liquid encapsulated floating zone technique for space processing of highly pure semiconductors has been proposed in [6].

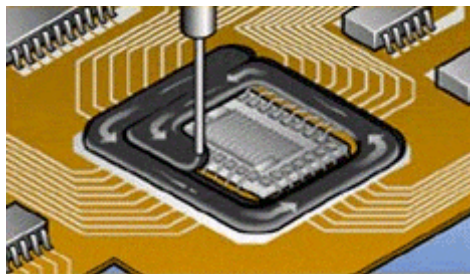


Figure 1. Encapsulation was jetted onto 3-mm parts.

It is well known that, the flow driven by a temperature gradient perpendicular to the interface is called Marangoni convection. However, thermocapillary convection is driven by the gradient of interfacial tension induced by the temperature gradient on the interface.

The thermocapillary convection in a multi-layer system has been extensively studied theoretically, experimentally and numerically. An extensive review of such investigations can be found in [7-16].

From the numerical point of view, it can be concluded that most of the previous investigations have neglected the deformation of the separation surface between liquid layers as a result of the complexity encountered in such simulations. Moreover, the satisfying of the interfacial boundary conditions on such moving interface is a challenge task. In a few studies, the dynamics of the deformable interface separating two layers was first computed using domain mapping in conjunction with a finite-difference scheme on a staggered grid [11].

Moreover, most of the previous investigations dealt with steady thermocapillary convection with small Marangoni number. Only few investigations have interested in the transition from steady to oscillatory convection with chaotic feature, e.g. [17, 18]. These investigations concerned only with the starting period of a complete route to turbulence, which is dependent on typical parameters such as Reynolds number, Prandtl number and geometrical aspects. At sufficiently high values of Marangoni number the flow exhibits oscillatory fluid motion and eventually becomes turbulent.

Consequently, in the present paper, the numerical investigations of turbulent thermocapillary convection are performed and the failure criterion of encapsulated chips is visualized.

2. Physical and Mathematical Models

The physical model of the encapsulated chips consists of a differentially heated rectangular cavity containing two immiscible liquid layers, as shown in Fig.2. The separation surface between

the two layers is assumed either fixed or deformable according to the case considered. Sketch of both cases can be seen in Fig.2. The side walls are kept at constant temperature with temperature difference of $\Delta T = T_{\text{hot}} - T_{\text{cold}}$. Other walls are assumed adiabatic.

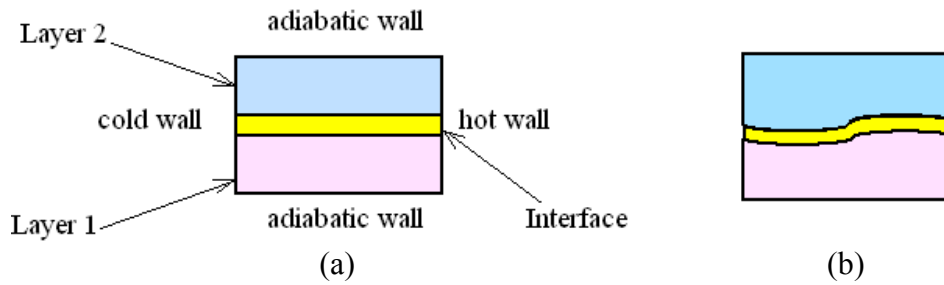


Figure 2. Physical model of two-layer system with (a) fixed interface, (b) deformable interface.

In the mathematical model, shown in Fig.3, it is assumed that the cavity has a length of L m and a total height $H = H_1 + H_2$ corresponding to the two immiscible layers.

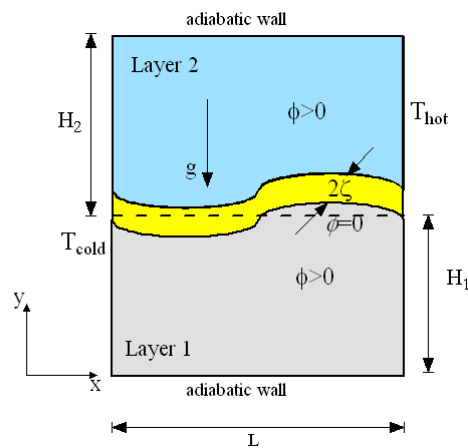


Figure 3. Mathematical model of two-layer system.

The interface thickness is assumed to be 2ζ . The initial interface is assumed to be flat and pinned to the side walls. In case of including the gravity force, it is assumed to be in the negative direction of y -axis. Upper and Lower walls are adiabatic, while the differential heating is parallel to the interface. The properties of each layer are characterized by the subscript 1 and 2, respectively.

2.1. Level set formulation

The level set formulation is applied in order to deal numerically with the problem of two immiscible fluids. The level set method is a class of capturing method where a smooth phase function, ϕ , is defined over the complete computational domain. In such a manner that at any given point, it is taken as the signed normal distance from the interface separates the two fluids with positive on one side (i.e. $\phi > 0$), and negative on the other (i.e. $\phi < 0$), as shown in Fig. 3. Consequently, the interface is implicitly captured as the zero level set of the level set function. This level set function is transported according to the calculated velocity field in both layers. The level set equation is described as follows:

$$\frac{\partial \phi}{\partial t} + \bar{u} \cdot \nabla \phi = 0 \quad (1)$$

where \bar{u} is the velocity vector. Consequently, the normal vector and the curvature of the interface can be defined as:

$$\bar{n} = \frac{\nabla \phi}{|\nabla \phi|}, \quad \kappa = \nabla \cdot \bar{n} \quad (2)$$

In order to overcome the problem of properties-discontinuity, which can arise in two immiscible layers, the fluid property, e.g. η , is smoothed across a finite thickness region of the interface [19];

$$\eta(\phi) = \eta_1 + (\eta_2 - \eta_1)H(\phi) \quad (3)$$

where η_1, η_2 are the values of the fluid property in the corresponding layer. The smoothed Heaviside function $H(\phi)$ is expressed as [20]:

$$H(\phi) = \begin{cases} 0 & \phi < -\zeta \\ 0.5[1 + \phi/\zeta + \sin(\pi\phi/\zeta)/\pi] & |\phi| \leq \zeta \\ 1 & \phi > +\zeta \end{cases} \quad (4)$$

with ζ the half-thickness of the transition region between layers, as shown in Fig. 3. The interface thickness is assumed to be 2ζ . The initial interface is assumed to be flat and pinned to the side walls. In order to maintain the level set function as a distance function within the two fluids at all times, especially near the interface region, the Eikonal equation, $|\nabla \phi| = 1$, should be satisfied in the computational domain. That can be achieved by applying the re-initialization algorithm described in [20].

Since the development of the level set method for incompressible two-phase viscous flows [20], a large amount of articles on the subject has been published and several types of problems have been tackled with this method; see for instance the cited review [21]. However, the implementation of the level set method in predicting the failure criterion of encapsulated chips and semiconductors is indeed new. Moreover, on the basis of the control volume approach and in turbulent flow regime, the problem of the thermocapillary convection in two-immiscible layers is indeed scarce.

2.2. Reynolds-Averaged Navier-Stokes equations

In the turbulent thermocapillary convection flow in two immiscible layers, the flow is governed by the Reynolds form of the continuity, momentum and energy equations for unsteady, incompressible and Newtonian flow. Following the Reynolds averaging procedure [22], the governing equations of turbulent flow based on the standard $k-\varepsilon$ model of [23] can be written as follows:

$$\frac{\partial(\rho u_i)}{\partial x_j} = 0 \quad (5)$$

$$\frac{\partial(\rho \bar{u}_i)}{\partial t} + \frac{\partial(\rho \bar{u}_i \bar{u}_j)}{\partial x_j} + \frac{\partial p}{\partial x_i} = \frac{\partial}{\partial x_j} \left[\mu \left(\frac{\partial \bar{u}_i}{\partial x_j} + \frac{\partial \bar{u}_j}{\partial x_i} \right) - \overline{\rho u'_i u'_j} \right] + (\sigma \kappa \bar{n} + \nabla_s \sigma) \delta(\phi) - g_i \beta (T - T_{ref}) \quad (6)$$

$$\frac{\partial(\rho T)}{\partial t} + \frac{\partial(\rho \bar{u}_j T)}{\partial x_j} = \frac{\partial}{\partial x_j} \left[\frac{\mu}{Pr} \frac{\partial T}{\partial x_j} - \overline{\rho u'_j T'} \right] \quad (7)$$

$$\frac{\partial(\rho k)}{\partial t} + \frac{\partial(\rho k \bar{u}_j)}{\partial x_j} = \frac{\partial}{\partial x_j} \left[\frac{\partial k}{\partial x_j} \left(\mu + \frac{\mu_t}{Pr_k} \right) \right] + (P_k + G_k) - \rho \varepsilon \quad (8)$$

$$\frac{\partial(\rho \varepsilon)}{\partial t} + \frac{\partial(\rho \varepsilon \bar{u}_j)}{\partial x_j} = \frac{\partial}{\partial x_j} \left[\frac{\partial \varepsilon}{\partial x_j} \left(\mu + \frac{\mu_t}{Pr_\varepsilon} \right) \right] + \frac{\varepsilon}{k} [C_{1\varepsilon} (P_k + G_k) - C_{2\varepsilon} \rho \varepsilon] \quad (9)$$

In the above system of equations, ρ is the density, \bar{u} is the velocity vector, p is the static pressure, σ is the surface tension coefficient, T is the temperature, \bar{q} is the heat flux vector, μ is the molecular viscosity, μ_t is the turbulent viscosity, k is the turbulent kinetic energy and ε is the turbulent dissipation.

The turbulent Reynolds stress is given by:

$$-\rho \overline{u'_i u'_j} = -\frac{2}{3} \rho k \delta_{ij} + \mu_t \left(\frac{\partial \bar{u}_i}{\partial x_j} + \frac{\partial \bar{u}_j}{\partial x_i} \right) \quad (10)$$

where δ_{ij} is the kronecker delta and $\overline{u'_i u'_j}$ is the average of the velocity fluctuations. The turbulent viscosity is defined as:

$$\mu_t = \rho C_\mu k^2 / \varepsilon \quad (11)$$

The coefficients for the standard turbulence model are given as follows [23]:

$$C_\mu = 0.09, Pr_k = 1, Pr_\varepsilon = 1.3, C_{1\varepsilon} = 1.44, C_{2\varepsilon} = 1.92$$

The turbulent Prandtl number is $Pr_t = 0.9$, while the molecular Prandtl number Pr and the specific heat capacity at constant pressure are defined according to the different layers considered. The additional term, G_k in k and ε equations is due to the representation of the buoyancy term and it is given by:

$$G_k = -g_i \beta \overline{u'_i T'} = -\frac{\mu_t}{Pr_t} \bar{g} \beta \nabla T \quad (12)$$

The production term of the turbulent kinetic energy is given by:

$$P_k = -\overline{u'_i u'_j} \frac{\partial u_i}{\partial x_j} \quad (13)$$

The Boussinesq approximation is employed in the last term of Eq. (6) where $T_{ref} = 0.5(T_{hot} + T_{cold})$ is a reference temperature, g_i is the gravitational acceleration vector and β is the thermal expansion coefficient.

In the present study, we apply the continuum surface force (CSF) model proposed by [24], where the interfacial jump conditions at the interface are modeled as a continuous force across the interface. Consequently, the interfacial jump conditions can be integrated into the momentum equation of a single incompressible fluid with variable properties, resulting in a body force concentrated in the interface, i.e.:

$$f_\sigma = (\sigma \kappa \bar{n} + \nabla_s \sigma) \delta(\phi) \quad (14)$$

where σ is the surface tension coefficient, $\delta(\phi)$ is delta function defined as $\delta(\phi) = dH(\phi)/d\phi$ [20]. The first term on the right hand side of the above equation represents the normal force resulting from the surface tension, while the second term stands for the tangential stress due to gradients of surface tension or Marangoni effect [25], usually important when large gradient of surface tension is present along the interface. The gradient tangential to the interface is defined using the tangential surface operator ∇_s . In thermocapillary convection, the surface tension gradient is related to the temperature gradient via the linear relation:

$$\sigma(T) = \sigma_{ref} - \gamma(T - T_{ref}) \quad (15)$$

where σ_{ref} is the surface tension at the reference temperature of the interface T_{ref} , and

$$\nabla_s \sigma = \sigma_T \nabla_s T \quad (16)$$

Consequently, the interfacial Marangoni number is defined as [8]:

$$Ma_t = \sigma_T \frac{\Delta T H_1^2}{\mu_1 \alpha_1 L} \quad (17)$$

where σ_T is the rate of change of surface tension according to the temperature change, described in [8], and α_1 is the thermal diffusivity of the corresponding layer.

2.3. Numerical Procedure

The numerical procedure adopted here is essentially based on the finite volume method proposed by Patankar [26]. For later convenience and dropping the overbar on the mean variables the Reynolds-averaged equation can be written in the following generic transport equation form:

$$\frac{\partial(\rho\phi)}{\partial t} + \frac{\partial(\rho u\phi)}{\partial x} + \frac{\partial(\rho v\phi)}{\partial y} = \frac{\partial}{\partial x}(\Gamma_\phi \frac{\partial\phi}{\partial x}) + \frac{\partial}{\partial y}(\Gamma_\phi \frac{\partial\phi}{\partial y}) + S_\phi \quad (18)$$

where the ‘‘scalar’’ variable ϕ , the diffusion coefficient Γ_ϕ and source term S_ϕ in the respective governing equation are appropriate for each variable (u , v , T , k , ϵ), see for more details [26].

In brief, for each variable, the above general differential transport equations is converted to algebraic equations before being solved numerically. The control volume formulation over a staggered grid system, which involves integrating the governing equations about each control volume, yielding discrete equations that conserve each quantity on a control-volume basis, is applied. The governing equations are discretized using the second-order upwind scheme to achieve the best accuracy. Pressure–velocity coupling was achieved using the SIMPLE algorithm [26]. The resulting equations are solved using TDM algorithm [22].

The segregated algorithm includes the following steps. First, the fluid properties are initialized according to the fluid layers considered. The momentum equations, subjected to well known boundary conditions, as shown in Fig.3, are then solved to obtain the velocity field using current values for pressure and mass fluxes. The continuity equation was then locally updated and corrected using the pressure correction derived from the continuity equation and the linearized momentum equations. The pressure correction equation is then solved to obtain the necessary corrections to the pressure and velocity fields and the mass fluxes. Finally, equations for temperature and turbulence are solved using the previously updated values of the other variables. In the level set method implemented, the momentum equations are solved throughout the domain, and the resulting velocity field is shared among the phases. The fluid–fluid interface during the calculation is updated in all of the interface cells by solving the transport equation of the level set function. Stable transient solutions were obtained with relatively small time steps, typically between 10^{-3} and 10^{-4} s.

The level set method equation is solved using the numerical scheme described in our previous work [27]. This scheme was validated and its accuracy was estimated against some pure translation test cases for interfaces with different shapes. More details about the numerical scheme used for the transport level set function and the appropriate validation cases can be found in [27].

3. Verification of the Numerical Method

In the following sections, a verification of our developed numerical scheme has been carried out by performing different benchmark problems containing two immiscible liquid layers.

3.1. Two Immiscible Liquid Layers in a closed Cavity (fixed Interface)

The first test case performed in this section is concerned with a numerical study of the flow characteristics of thermocapillary convection in a system composed of two immiscible liquid layers subjected to a temperature gradient along their interface. The two-layer system

consists of B_2O_3 (encapsulant) and GaAs (melt) with physical properties defined in [10]. The liquid-liquid interface is assumed to be undeformable and flat, which is a valid assumption according to earlier theoretical and experimental results.

Fig. 4 shows the obtained numerical results of the dimensionless horizontal velocity profile at $x=0.5L$ for a system with aspect ratio of $A=L/H_2=4$ when compared with the analytical solution of [10]. The dimensionless velocity is obtained using the quantity α_2/H_2 . The system is considered to be symmetrical in layers properties and depth, i.e. ($H_1=H_2$) with Marangoni number $Ma=3750$. The obtained numerical results showed a good agreement with the analytical solution.

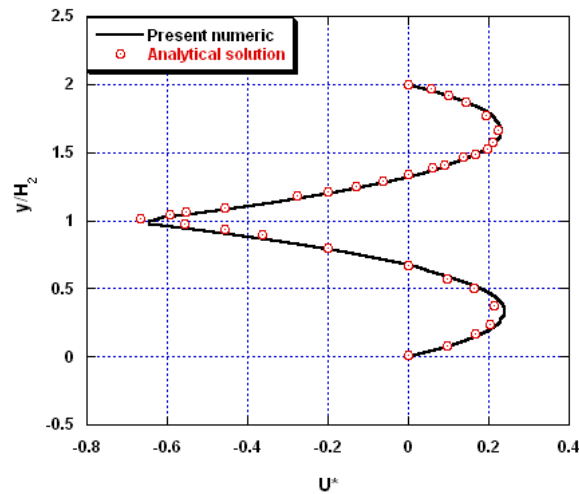


Figure 4. The dimensionless horizontal velocity profile for symmetrical system compared with the analytical solution of [10].

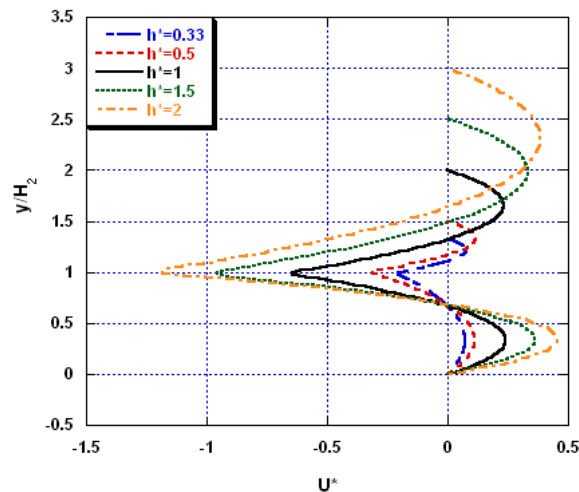


Figure 5. Effect of increasing layers thickness on the dimensionless horizontal velocity.

Fig.5. shows the effect of altering the thickness ratio H_1/H_2 . The melt layer depth (H_1) is kept constant, while the thickness of encapsulant is varied from 0.33 to 2. It can be seen that, the convective flow, either in the encapsulant or in the melt, becomes less and less strong when h^* decreases.

3.2. Oscillation of inviscid capillary waves

One of the most important as well as interesting problems in hydro-dynamical theory is the oscillation of a free surface under surface tension effect. The linear theory provided by [28]

described the small amplitude oscillation of an interface between two inviscid fluids of equal density. Assuming an arbitrary interface between superposed inviscid fluids having an infinitesimally small and horizontal sinusoidal displacement, as a result of random disturbances, is imposed upon the initially steady free surface. The initial free surface has the form:

$$\eta(x, t) = \eta_o \cos(\omega t + kx) \quad (19)$$

where η represents the displacement of the free surface in the vertical direction from its undisturbed position, η_o is the initial amplitude, t is time, $k=2\pi/\lambda$ is the wave number, λ is the wavelength, and ω is the excitation frequency. The initial frequency of the oscillation is given by the following relation:

$$\omega_o = \sqrt{\frac{\sigma k^3}{2\rho}} \quad (20)$$

The sinusoidal perturbation is assumed to divide horizontally a square box in two equal parts, i.e. the width of the tank is twice the depth of the still water level which allowed oscillating freely. The sinusoidal perturbation is considered to have a wavelength equals to the box width and an initial amplitude of $\eta_o/\lambda = 0.01, 0.001$ and $\eta_o = 0.005$.

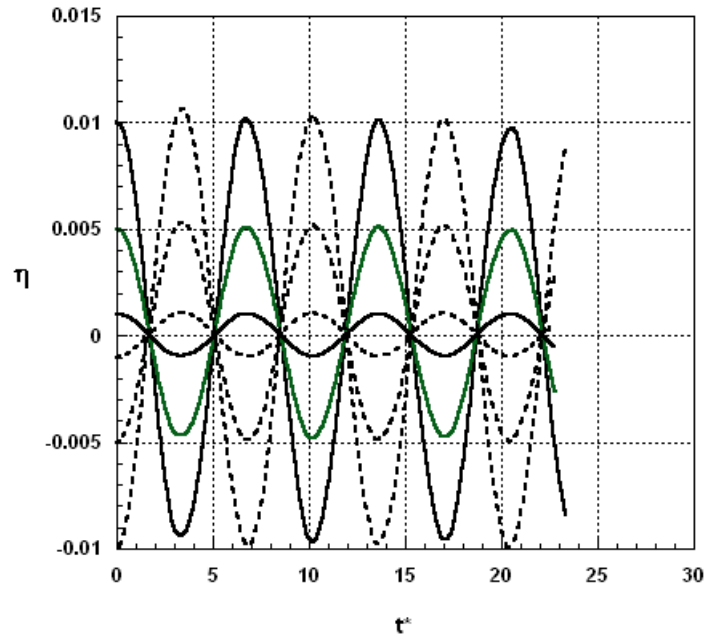


Figure 6. Evolution of inviscid capillary wave amplitude on the left wall (—) and on the middle of the tank (-----) for different initial amplitudes.

As can be seen in Fig. 6, no excessive damping of the free surface elevation could be observed over a large period of time. Moreover, the constant period of oscillation reveals that a good mass conservation has been obtained using the prescribed algorithm of the level set method. In general, it can be stated that our numerical method predicts the amplitude evolution of the inviscid capillary wave with good accuracy compared with the results of [29], where a decay of the inviscid wave amplitude is observed.

3.3. Two Immiscible Liquid Layers in a closed Cavity (moving Interface)

Let us consider now that the separation surface between the two layers is allowed to deform. The numerical experiment performed by [8] is now carried out in this section. The layers properties are taken as those considered in [8]. Fig.7 shows the effect of viscosity ratio between two layers on the interface deformation. When the viscosity of the upper layer is greater than

that of the lower layer, the larger pressure in the encapsulant layer near the cold wall causes the interface to dip into the melt, while the smaller pressure in the encapsulant layer near the hot end gives rises protrusion of the interface into the encapsulant layer. In contrary, when the viscosity of the upper layer is smaller than that of the lower layer, the interface deformation gives a reverse behavior.

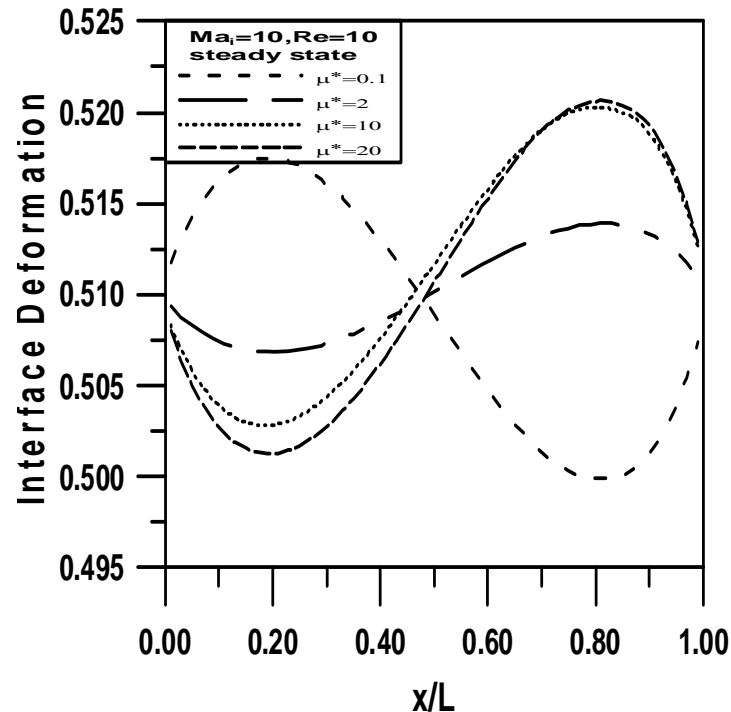


Figure 7. Interface Deformation with $Ma_i=10$, $Re=10$, $Pr=1$, $a^*=1.0$ and $A=1$.

3.4. Turbulent Natural Convection in a square Cavity

In this section, we predict the turbulent natural convection of a single phase in a square cavity. The obtained results are compared with the experimental measurements of [30]. Fig. 8 shows a comparison between the present predicted Nusselt numbers calculated at both of cold and hot wall of the square cavity and those measured by [30]. It can be seen that, the calculated Nusselt number agrees well with the experimental measurement especially near the side walls. However, near the centre of the cavity, it can be seen some deviation from the experimental measurements due to the difficulties encountered in the experimental measurements [30].

Fig. 9 shows another comparison for the distribution of the dimensionless temperature calculated at the middle of the cavity ($x/L=0.5$) and compared with the experimental measurements of [30]. In general, fairly agreement was obtained, however, some discrepancies could be observed near the upper and lower walls due to the turbulence model applied in this study. It is expected that good agreement could be obtained by application of more reliable turbulence model, e.g. Low Reynolds $k-\epsilon$ turbulence model. For more details, one can see [31].

4. Results and Discussion

Thermocapillary convection in an encapsulated chip and semiconductors becomes very important when ever a strong temperature gradient is present over the interface separating the two layers. By increasing the temperature gradient the Marangoni number exceeds a critical value and periodic and non-periodic oscillations are expected. Consequently, the flow becomes unstable and small perturbations can be amplified, leading to transition to turbulence when they exceed a critical finite amplitude.

The simplest configuration used to study the turbulence effect is the problem of a rectangular cavity containing two immiscible liquid layers with top rigid surface. The interface dynamics is predicted either in case of negligible or allowed deformation. The computational domain consists of 201×101 grid points in x and y directions, respectively with a grid distance of $\Delta x = \Delta y = 1.02 \times 10^{-4}$ m. The two liquids considered have the same properties as described in [8]. The numerical simulation is performed for relatively higher Marangoni number in case of undeformed and deformed interface.

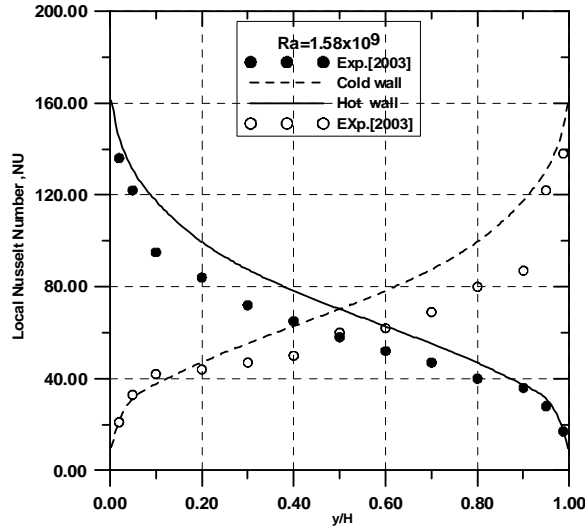


Figure 8. Local Nusselt number distribution for turbulent natural cavity.

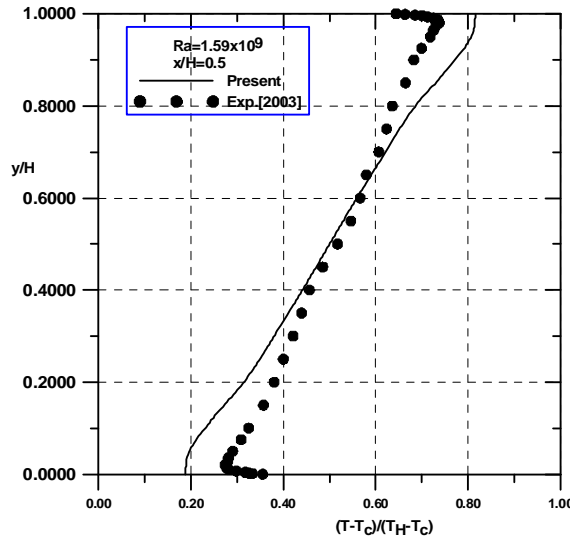


Figure 9. Dimensionless temperature distribution at $x/L=0.5$ for turbulent natural cavity.

Fig. 10 shows the dimensionless horizontal velocity profile at $x/L=0.5$, plotted in the two layers for two different Marangoni numbers; $Ma_1=28500$ and $Ma_1=57000$. It is indicated that the amplitude of the interfacial velocity increases with increasing the Marangoni number. However, no indication about the transition to turbulent flow could be demonstrated. Even by increasing the Marangoni number to 114000 and plotting the streamlines in the two layers, as shown in Fig. 11, one can observe only a stronger convective cell in the lower layer with its center shifting towards the cold wall. This is a normal behavior by increasing the Marangoni number even in case of neglecting the turbulent effect.

From the above discussion, it can be concluded that the transition to turbulent could not numerically predicted by the assumption of undeformed interface. Consequently, we perform the above considered cases, however, with deformable interface. Fig. 12-a shows the surface plot of the

interface at $Ma_i=28500$ in a turbulent two-layer system. For such low Marangoni number the interface deforms almost in sinusoidal form with unequal wave amplitude. This is a similar deformation to the case of neglecting the turbulence effects and with the same Marangoni number (not presented here). However, by increasing the Marangoni number, i.e. $Ma_i=57000$ and more, the transition to turbulent is observed by indicating the irregular surface deformation arising near the hot wall. There a huge movement of the liquid in the melt layer which causes the strong deformation of the interface as a result of the large interfacial temperature gradient near the hot wall.

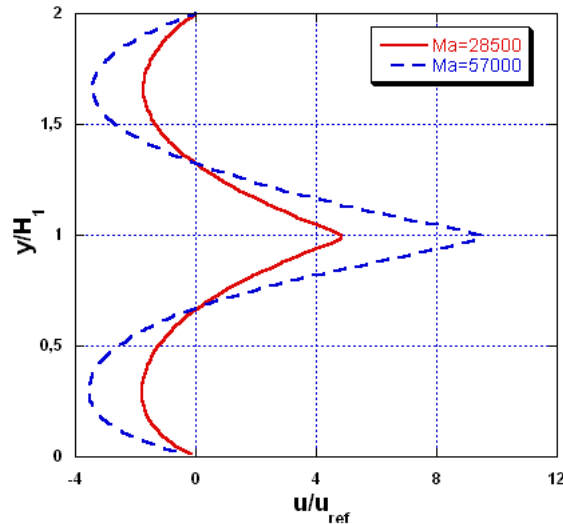


Figure 10. Dimensionless horizontal velocity profile at $x=0.5$ in a turbulent two-layer system with fixed interface at different Marangoni numbers.

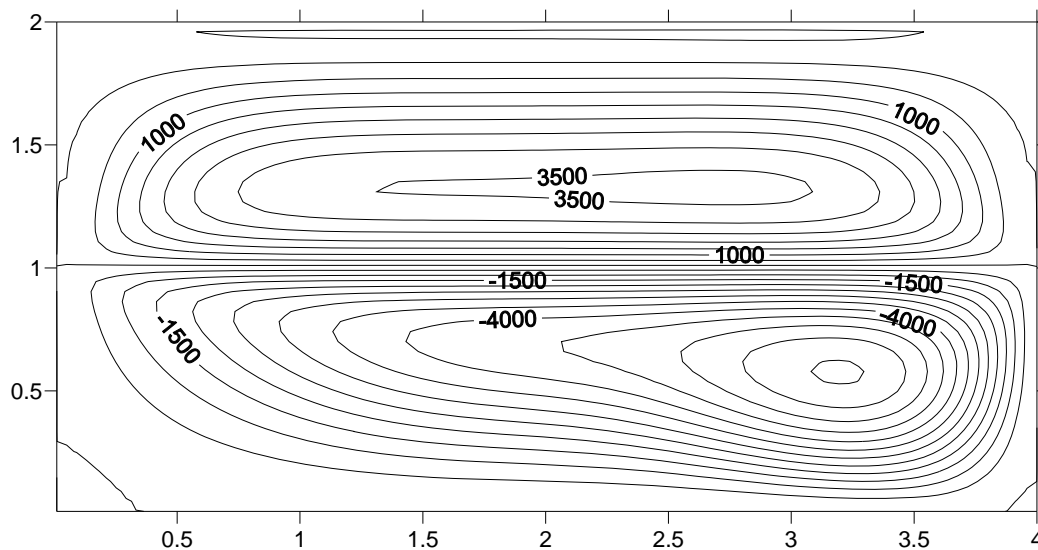


Figure 11. Streamlines for a turbulent two-layer system with fixed interface at high Marangoni number $Ma_i=114000$.

Fig. 12-b shows some kind of such irregular surface deformation that could be initiated in such cases. As a result of such deformation we refer the most failure characteristics of the viscous melt-encapsulant layered subjected to high differential temperature gradient.

By increasing the Marangoni number to $Ma_i=11400$, as shown in Fig. 13, a surface instability is observed in the encapsulated layer revealing the total failure of the chips and semiconductors. A detailed study should be performed in our future study to prevent such surface instabilities and to find out the thermal conditions as well as the layers properties preventing such instabilities.

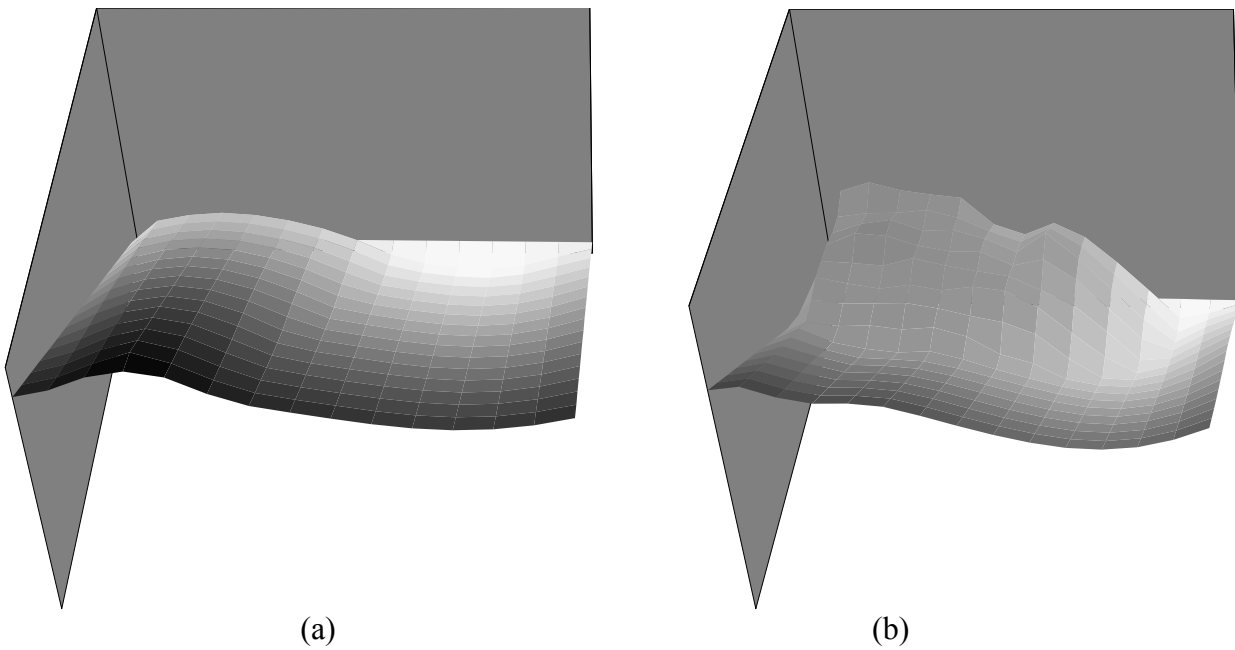


Figure 12. Interface deformation in a turbulent two-layered system at different Marangoni numbers (a) $Ma_i = 28500$, (b) $Ma_i = 57000$.

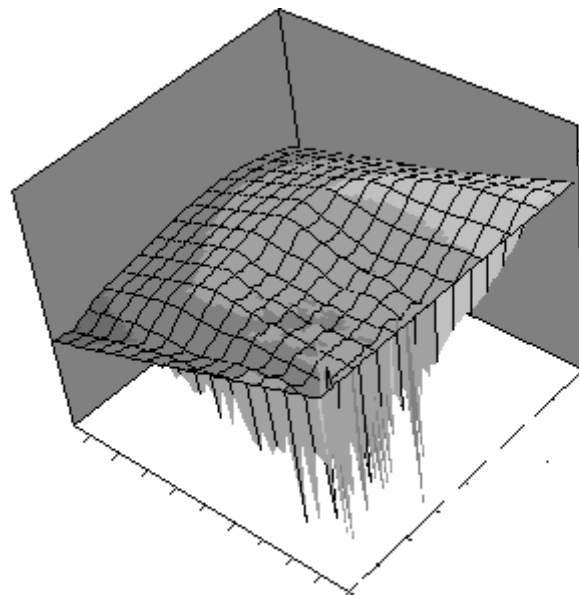


Figure 13. Interface deformation in a turbulent two-layered system Marangoni numbers $Ma_i = 114000$.

5. Conclusions

A numerical method is applied for predicting the failure characteristics of encapsulated chips and semiconductors due to high level of differential heating. The level set method is coupled with the RANS equation to predict such effects. The numerical results are validated firstly against different test cases. For the a turbulent two-layer system, the transition to turbulent flow is associated with the assumption of moving interfaces only and that could not be predicted in case of fixed interface assumption. The transition to turbulent flow is related, of course, to the properties of the double-layer materials. An irregular interface deformation has been numerically predicted by increasing the Marangoni number in the near of the hot wall. A detailed investigation considering the effect of fluids properties on the transition Marangoni numbers is required in a future study.

References

- [1] Wunderle, B.; Mrossko, R.; Kaulfersch, E.; Wittler, O.; Ramm, P.; Michel, B. and Reichl, H., *Thermo-Mechanical reliability of 3D-Integrated structures in stacked silicon*, Proc. MRS Fall Meeting, Boston, USA; Nov. 2006.
- [2] Nepomnyashchy, A.A.; Simanovskii, I.B.; Legros, J.-C., *Interfacial Convection in Multilayer Systems*, Springer, New York; 2006.
- [3] Liu, Q.S.; Hu, W.R.; Roux, B., *On the convective flow of multi-layer liquids*, *Advances in Mechanics* 1997; 27: 518-537.
- [4] Metz, E.P.A.; Miler, R.C.; Mazelsky, R., *A technique for pulling single crystals of volatile materials*, *J. Applied Physics* 1962; 33:2016-2017.
- [5] Johnson, E.S., *Liquid encapsulated floating zone melting of GaAs*, *J. Crystal Growth*, 1975; 30:249-256.
- [6] Balocela, E.; and Jalilevand, A., *Liquid encapsulated float zone method for microgravity production of gallium arsenite*, *AIAA* 1987; 87-0390.
- [7] Langlois, W.E., *Buoyancy-driven flows in crystal-growth melts*, *Ann. Rev. Fluid Mech.*, 1985; 17:191-215.
- [8] Doi, T.; and Koster, J.N., *Thermocapillary convection in two immiscible liquid layers with free surface*, *Phys. Fluids* 1993; A 5: 1914–1927.
- [9] Prakash, A.; and Koster, J. N., *Steady natural convection in a two-layer system of immiscible liquids*, *International Journal of Heat and Mass Transfer* 1997; 12:2799-2812.
- [10] Liu, Q.S.; Roux, B.; Velarde, M.G., *Thermocapillary convection in two-layers system*, *Int. J. Heat Mass Transfer* 1998; 41: 1499–1511.
- [11] Gupta, N.R.; Haj-Hariri, H.; Borhan, A., *Thermocapillary flow in double-layer fluid structures: an effective single-layer model*, *J. Colloid Interface Sci.* 2006; 293: 158–171.
- [12] Gupta, N.R.; Haj-Hariri, H.; Borhan, A., *Thermocapillary convection in double layer fluid structures within a two-dimensional open cavity*, *J. Colloid Interface Sci.* 2007; 315:237–247.
- [13] Abidin, N. Z.; Arifin, N. M. and Noorani, M. S. M., *Boundary effect on Marangoni Convection in a Variable Viscosity Fluid Layer*, *Journal of Mathematics and Statics* 2008; 1:1–8.
- [14] Li, Y.; Wang, S.-C.; Wu, S.-Y. and Peng, L., *Asymptotic solution of thermocapillary convection in thin annular two-layer system with upper free surface*, *International Journal of Heat and Mass Transfer* 2009; 52:4769–4777.
- [15] Ueno, I.; and Torii, T., *Thermocapillary-driven flow in a thin liquid film sustained in a rectangular hole with temperature gradient*, *Acta Astronautica* 2010; 66: 1017–1021.
- [16] Pendse, B.; and Esmaeeli, A., *An analytical solution for thermocapillary-driven convection of superimposed fluids at zero Reynolds and Marangoni numbers*, *International Journal of Thermal Sciences* 2010; 49:1147-115.
- [17] Ward, C.A.; and Duan, F., *Turbulent transition of thermocapillary flow induced by water evaporation*, 2004; E69:1-10.
- [18] Das, K. S.; MacDonald, B. D.; Ward, C. A., *Stability of evaporating water when heated through the vapor and the liquid phases*, *phys. Rev.* 2010; E81:1-14.
- [19] Carrica, P. M.; Wilson, R. V. and Stern, F., *An unsteady single-phase level set method for viscous free surface flows*, *Int. J. Num. Meth. Fluids* 2007; 53: 229–256.
- [20] Sussman, M.; Smereka, P.; and Osher, S. J., *A Level set Approach to Computing Solutions to Incompressible Two-Phase Flow*, *J. Comp. Phys.* 1994; 114:146-159.
- [21] Sethian, J. A.; and Smereka, P., *Level set Methods for Fluid Interfaces*, *Annu. Rev. Fluid Mech.* 2003; 35:341-372.
- [22] Anderson, D. A.; Tannehill, C. J.; and Pletcher, R. H., *Computational Fluid Mechanics and Heat Transfer*, Hemisphere Publishing Corporation; 1984.

- [23] Launder, B.E.; and Spalding, D.B., *The numerical computation of turbulent flow*, Computer Methods in Applied Mechanics and Engineering 1974;2:269-289.
- [24] Brackbill, J. U.; Kothe, D. B.;and Zemach, C. A. , *A Continuum Method for Modeling Surface Tension*, J. Comput. Phys. 1992; 100:335-354.
- [25] Marangoni, C., *Über die Ausbreitung der Tropfen einer Flüssigkeit auf der Oberfläche einer Anderen*, Annual Physical Chemistry 1871; 143:337-354.
- [26] Patankar, S. V., *Numerical Heat Transfer and Fluid Flow*. Hemisphere Publishing Corporation; 1980.
- [27] Balabel, A.; Binninger, B.; Herrmann, M. and Peters, N., *Calculation of Droplet Deformation by Surface Tension Effects using the Level Set Method*, J. Combustion Science and Technology 2002; 11-12: 257-278.
- [28] Landau, L.D.; and Lifshitz, E.M., *Fluid Mechanics*, Pergamon Press, New York, 1959.
- [29] Iafrafi, A.; Di Mascio, A. and Campana, E.F., *A level set technique applied to unsteady free surface flows*,Int. J. Numer. Meth. Fluids 2001; 35: 281–297.
- [30] Karayiannis, A. F.; and T.G., *Experimental benchmark data for turbulent natural convection in an air filled square cavity*, Int. J. Heat and Mass Transfer 2003; 46: 3551-3572.
- [31] Hsieh, K.J.; and Lien, F.S., *Numerical modeling of buoyancy-driven turbulent flows in enclosures*, International Journal of Heat and Fluid Flow 2004; 25:659–670.